

Control of mobility in molecular organic semiconductors by dendrimer generation

J. M. Lupton,^{1,2} I. D. W. Samuel,^{1,2*} R. Beavington,³ M. J. Frampton,³ P. L. Burn,³ and H. Bässler⁴

¹*School of Physics and Astronomy, University of St. Andrews, St. Andrews, Fife KY16 9SS, United Kingdom*

²*Department of Physics, University of Durham, South Road, Durham DH1 3LE, United Kingdom*

³*The Dyson Perrins Laboratory, University of Oxford, South Parks Road, Oxford OX1 3QY, United Kingdom*

⁴*Institute of Physical Chemistry, University of Marburg, Hans-Meerwein-Strasse, D-35032 Marburg, Germany*

(Received 15 August 2000; revised manuscript received 15 November 2000; published 30 March 2001)

Conjugated dendrimers are of interest as novel materials for light-emitting diodes. They consist of a luminescent chromophore at the core with highly branched conjugated dendron sidegroups. In these materials, light emission occurs from the core and is independent of generation. The dendron branching controls the separation between the chromophores. We present here a family of conjugated dendrimers and investigate the effect of dendron branching on light emission and charge transport. We apply a number of transport measurement techniques to thin films of a conjugated dendrimer in a light-emitting diode configuration to determine the effect of chromophore spacing on charge transport. We find that the mobility is reduced by two orders of magnitude as the size of the molecule doubles with increased branching or dendrimer generation. The degree of branching allows a unique control of mobility by molecular structure. An increase in chromophore separation also results in a reduction of intermolecular interactions, which reduces the red emission tail in film photoluminescence. We find that the steady-state charge transport is well described by a simple device model incorporating the effect of generation, and use the materials to shed light on the interpretation of transient electroluminescence data. We demonstrate the significance of the ability to tune the mobility in bilayer devices, where a more balanced charge transport can be achieved.

DOI: 10.1103/PhysRevB.63.155206

PACS number(s): 73.61.Ph, 36.20.-r, 85.60.Jb, 72.80.Le

I. INTRODUCTION

Studies of the nature of charge transport in highly disordered organic semiconductors have experienced a renaissance since the discovery of efficient electroluminescence (EL) in small organic molecules¹ and polymers.² Progress on materials and devices has led to a vast array of electronic and optoelectronic applications.³ Most organic materials have low mobilities in comparison to their inorganic counterparts and, hence, there has been considerable interest in increasing these mobilities to find materials capable of sustaining the currents required for field-effect transistors and organic lasers.⁴⁻⁷ Generally, mobilities in amorphous films of polymers or organic molecules are rather low when compared to crystalline materials. Although there have been attempts to correlate the chemical and physical structure of organic materials with their mobilities, little is known about which of the numerous mechanisms of mobility lowering such as phonon scattering, hopping, or trapping, is the dominant process in common organic EL materials. There is also no clear strategy on how to tune the mobility of organic semiconductors. Conjugated polymers in particular do not lend themselves readily to structural studies due to their inherent disorder, and many previous discussions have hence been based on stochastic models.^{8,9} The charge-carrier mobility in luminescent polymers is related to the chemical structure of the polymer and the microscopic conformation. Martens, Blom, and Schoo have used the concept of energetic disorder to explain the wide range of mobilities observed in a recent comparison of different PPV-based polymers.¹⁰ In contrast, a geometrical model has been invoked to explain the large difference in mobilities between highly disordered materials such as MEH-PPV and more rigid polymers such as polyfluorenes.¹¹

Conjugated dendrimers can consist of an emissive core region and branching units, termed dendrons, of higher band gap that give rise to exciton localization on the core. Emission hence occurs from the core and can be controlled independently of the dendron architecture. We demonstrate below that the dendron periphery of conjugated dendrimers acts as spacers between the emissive units of the molecules, and the number of branching points of the dendrons allows a microscopic control of the interchromophore separation. This control of the interaction between individual chromophores allows an unambiguous study of the effect of molecular arrangement on the transport properties within the organic material. In addition, we find a direct correspondence between the charge transport properties and the photophysical properties.

In this paper, we consider conjugated dendrimers formed from a propellerlike arrangement of a conjugated core and stilbene-based dendrons, where the electron delocalization is broken between the core and the dendron regions by the meta linkages. The degree of branching of the dendron units is described by the dendrimer generation, as seen in Fig. 1 (to be discussed further on). Electroactive dendrimers have been studied in a number of contexts¹²⁻¹⁹ including their use as charge transporting or emissive layers in organic light emitting diodes (LEDs). It has been suggested that the dendrons can act as funnels for excitations, guiding these to the core and, hence, giving strong localization.²⁰ The dendrons can also act as protective shields to the environment. In devices, however, it appears that dendrons can act as insulating spacers between the chromophores.¹⁹ Dendrimers can be synthesized in an orderly manner such that the precise structure and molecular weight are known. This is in contrast to some polymers where batch-to-batch variations of the mo-

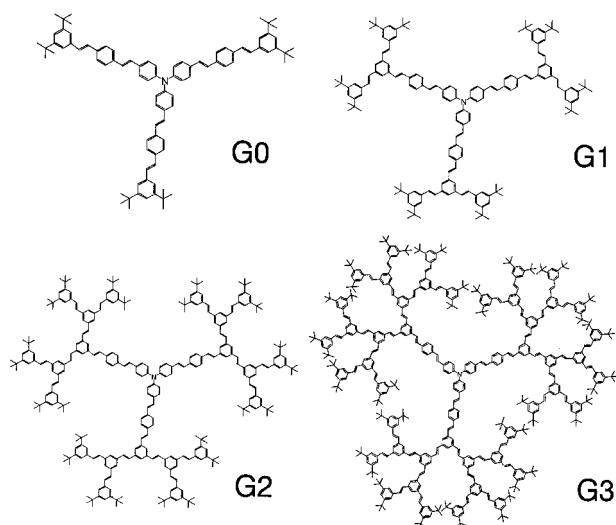


FIG. 1. Structures of the family of dendrimers of generation (G) 0 to 3.

molecular weight can occur. Batch-to-batch variations in polymer synthesis have been shown to give rise to dramatic variations of device properties,²¹ which greatly complicates attempts to relate the chemical structure to the charge transport in polymers. Conjugated dendrimers bridge the gap between small organic molecules and conjugated polymers. The core chromophore unit may be based on either small organic compounds such as porphyrins and anthracene, or oligomer units of commonly used polymers. The dendrimer generation can be exploited as a direct control of the spacing between the core units of the dendrimers.

The effect of chromophore spacing in films of organic materials is of both applied and fundamental interest. In the present case, the degree of dendron branching allows a direct control of this spacing and, hence, the level of intermolecular interaction. The level of interaction between the chromophores is of great importance: on the one hand, an increase in interaction due to a reduction in chromophore spacing is beneficial to the charge transport; on the other hand, interactions can lead to excimer or aggregate formation and luminescence quenching. An investigation of the trade-off between these two competing processes requires a way of controlling the spacing between molecules. Dendrimers provide a unique way of achieving this: by changing the generation, a direct control of the degree of shielding of the chromophore and, hence, the interchromophore spacing is achieved. The hopping distance between molecular sites controls the charge-carrier mobility. This control of mobility can then be used to test an LED device model and also lead to an improved understanding of the turn-on dynamics of LEDs. In the following section, we outline the experimental procedure. The Results section is split into five parts, describing the photophysics, mobility, device modeling, transient EL, and finally, a practical application of the control of mobility to efficient bilayer LEDs.

We employ here oligomer units of the widely used conjugated polymer PPV to investigate the effect of spacing between chromophores that is controlled by the dendrimer generation. The structures of the dendrimers studied of gen-

eration 0 to 3 are given in Fig. 1. Three distyrylbenzene units are grouped around a nitrogen atom, which, according to x-ray crystallography data on triphenylamines, should be in a nonplanar configuration.²² Stilbene units form the dendrons which are *meta* linked with respect to the distyrylbenzene and do not allow for electron delocalization from the core to the dendrons. *t*-Butyl surface groups terminate the dendrons and control the solubility of the material.

II. EXPERIMENT

The dendrimers are readily soluble in organic solvents such as tetrahydrofuran, toluene, and chloroform. Films were spin coated from tetrahydrofuran solutions of concentration 10 mg/ml. Photoluminescence (PL) spectra were measured under excitation from an Argon-ion laser at 351.1 and 363.8 nm using a charge-coupled device (CCD) spectrometer. Charge transport in the dendrimers was studied in films of thicknesses of typically 100 to 200 nm by time-of-flight (TOF), current-voltage measurements, and transient EL. TOF measurements^{23–30} were performed on films spin coated on an indium tin oxide (ITO) layer and coated with an evaporated 15 nm-thick rhodamine 6 G charge generation layer. Evaporated aluminum electrodes of area 1 mm² were used. Charge carriers were generated with a 10 ns laser pulse from a Nd:Yttrium aluminum garnet (Nd:YAG) laser driving an optical parametric oscillator at an output wavelength of 555 nm. The ITO electrode was negatively biased so that holes generated in the rhodamine 6 G layer traversed the dendrimer film to be annihilated at the ITO electrode, whereas electrons were rapidly removed from the device by the aluminum anode. The photocurrent transients, which hence correspond to hole currents, were measured using a storage oscilloscope.

Single-layer LEDs were fabricated on patterned ITO substrates etched in hydrochloric acid and cleaned in ultrasonic baths of acetone and subsequently 2-propanol. The counter electrode was aluminum (2 mm²) in the case of devices consisting of a single organic layer. Devices used in the study of single-layer current-voltage characteristics and device efficiency contained a PEDOT hole injecting layer³¹ between the dendrimer and the ITO. PEDOT was spin coated from water and subsequently dried at 80 °C under a vacuum for two hours. Current-voltage and efficiency measurements were performed using a Keithley source-measure unit. Transient EL measurements were carried out on devices with no PEDOT layer and active areas of 7 mm² using a photon counting setup to detect the emitted light. LEDs were driven by a commercial pulse generator with a rise time <10 ns. Bilayer devices were fabricated by vacuum deposition of an electron transporting layer of PBD or Alq₃ onto the dendrimer film. For these devices, only magnesium-aluminum cathodes were used and the substrates were not patterned. All measurements were performed under vacuum except for the measurements on bilayer devices, which were carried out on a separate experimental setup.

III. RESULTS AND DISCUSSION

A. Control of intermolecular interactions

The PL spectra of zeroeth (G0) and third (G3) generation dendrimers in film and tetrahydrofuran solution are shown in

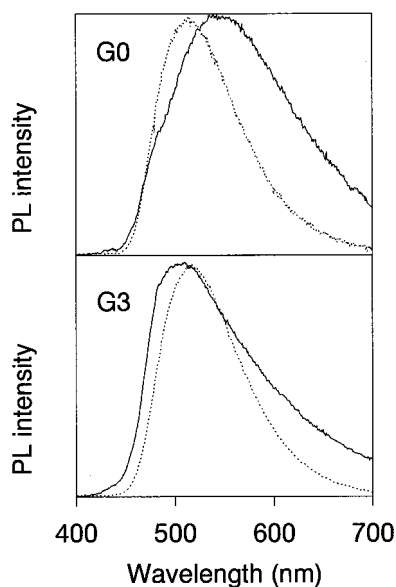


FIG. 2. PL spectra (excited at 365 nm) of dendrimers G0 and G3 in solution (\cdots) and film (—).

Fig. 2. The PL spectra of all four generations were measured in solution and film. The solution spectra of each generation are identical, whereas the film spectra differ strongly at longer wavelengths. The G0 film spectrum has a large red emission tail, which is much reduced in the G3 film emission. We do not observe a corresponding low-lying feature in the absorption spectra (not shown), and therefore assign the red tail to excimer emission, which is a well-known phenomenon in conjugated molecules.^{24,32–34} The emission spectra of intermediate generations lie in between these two extremes. We find that the difference between film and solution emission is reduced with increasing generation. As the dendrimer generation is increased, the distance between the chromophores increases and, hence, the possibility for excited state interactions is reduced. This results in a reduction of the red emission at higher generations. It is also seen that the G3 film emission is shifted slightly to the blue with respect to the solution emission, which we attribute to a twisting of the molecule in the film. The peak optical densities of the G0 solution studied (in a 1 cm quartz cuvette) and the film (100 nm thick on quartz discs) were 0.55 and 0.6, respectively. For G3, two absorption peaks are observed, corresponding to the core and the dendron absorption. The core absorbances are 0.024 and 0.1 in solution and film, respectively, whereas the dendron absorbances are 0.17 in solution and 0.6 in the film. Internal filter effects are not thought to contribute to the slight blue shift seen from solution to film luminescence, as the G3 film is optically denser than the solution, yet the film emission is shifted to the blue.

The photophysical properties presented above are a piece of evidence that the group of materials used here allows a direct control of the level of interaction between chromophores by spacing them further apart with increasing dendrimer generation. As will be seen in the following, there is a direct correspondence between the reduction in intermolecular interaction and the reduction in charge-carrier mobility of the material.

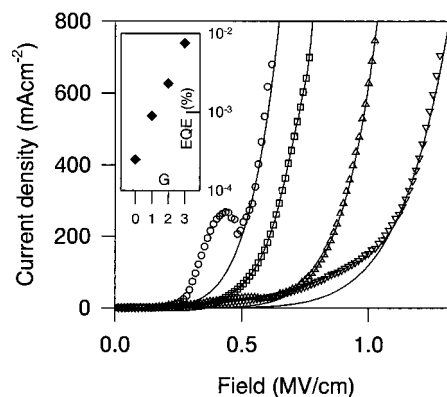


FIG. 3. Current-electric field characteristics of dendrimer LED's, from left to right, G0 (\circ), G1 (\square), G2 (\triangle), G3 (∇). Inset is the external quantum efficiency as a function of generation. The solid lines are model fits described in Sec. III C.

B. Control of mobility

The current-electric field characteristics of single-layer devices in the configuration ITO/PEDOT/dendrimer/Al are shown in Fig. 3. The solid lines correspond to model fits that are discussed in Sec. II C. It is seen that the operating field increases with increasing dendrimer generation, implying that the films become more insulating. The inset shows the EL external quantum efficiency (EQE) of LEDs as a function of generation. The EQE increases by a factor of 25 as the generation increases from 0 to 3. In contrast, we observe a much smaller little change in the solid state PL quantum yield with generation, suggesting that the rise in EQE is due to more balanced transport between electrons and holes with increasing generation.

We investigated the charge transport further by measuring the majority carrier mobility directly using the TOF technique. Triaryl-amine-based compounds are commonly used for hole transporting material, so we assume that in the case of these dendrimers, the majority carriers are holes. The hole-current transients were measured using a storage oscilloscope and were found to be subject to strong dispersion. The duration of the transients increases dramatically with generation. The photocurrent transients are well described by two power laws, following the conventional analysis of dispersive signals.²³ The transit time was determined by the point of inflection of the short- and long-time asymptotes of the transients on a double logarithmic representation. The mobility is derived from the transit time according to $\mu = d^2/V\tau$, where d is the film thickness, V is the applied bias, and τ is the transit time.

Two sample photocurrent traces for approximately 200 nm thick films of dendrimer generations G0 and G3 are seen in Fig. 4. The important observation is that the timescale over which the current decays increases by over an order of magnitude between G0 and G3. The traces are highly dispersive and no plateau is visible. However, the photocurrent decays according to a power law and two regions of distinct exponents can be identified and are marked in the figure with straight lines. The intersection of these lines allows an estimation of the transit time (0.8 and 14 μ s, for G0 and G3, respectively).

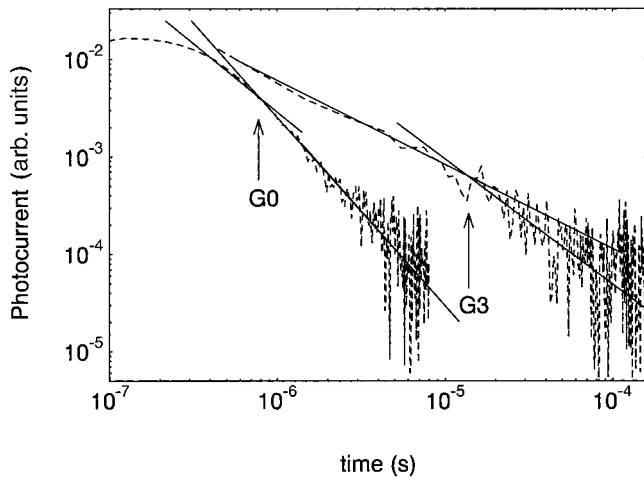


FIG. 4. Sample photocurrent transients of G0 and G3 at electric fields of 0.3 MV/cm and 0.9 MV/cm, respectively. The straight lines indicate the power-law decay of the photocurrent. The intersect of the two lines marks the transit time.

The mobility values are shown in Fig. 5 for the four generations of the dendrimer as a function of the applied field. (The lines correspond to mobility values derived from the fits in Fig. 3, as discussed in the following section.) As the generation increases, the charge-carrier mobility is reduced by almost two orders of magnitude, showing a clear correlation between the degree of dendron branching and the charge-carrier mobility. Also, the mobility shows an increase with the electric field of the Poole-Frenkel form characteristic of transport in disordered systems.⁸ We find that as the generation increases, the dielectric strength of dendrimer films increases, which defines the range of fields that may be applied to the films. In the low-field region the instrumental sensitivity poses limits on the measurable transit time, which explains the absence of lower-field values for G2 and G3. As the dendrimers become considerably larger with generation,

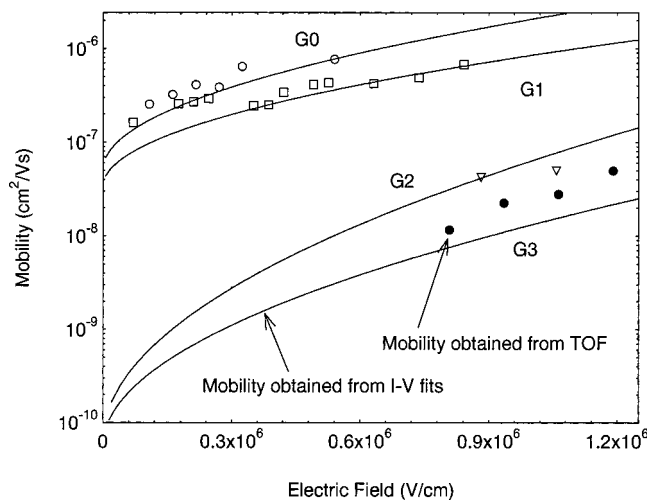


FIG. 5. Mobility values obtained for dendrimer films by time of flight measurement (data points). The lines are mobility values obtained from fits to the current-voltage characteristics seen in Fig. 3 and described in Sec. III C.

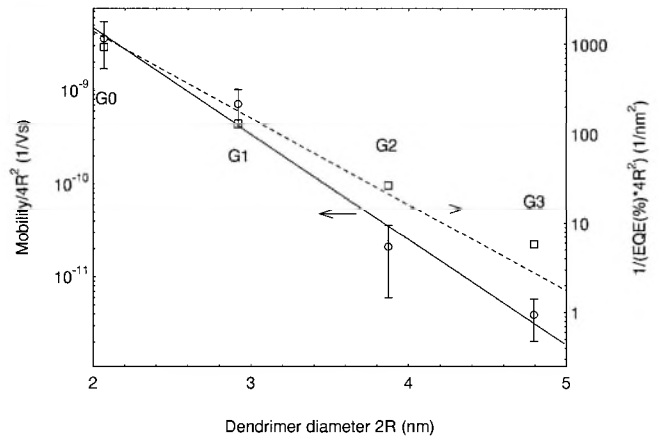


FIG. 6. Scaling of mobility (○) and device external quantum efficiency (□) with dendrimer radius.

the chromophore spacing increases with generation due to the increased fraction of insulating dendron units in the film. The situation resembles the case of molecularly doped polymers: the core of the dendrimer can be likened to the guest dopant dispersed in a host of stilbene dendrons. However, the generation of the dendrons provides a way of controlling the concentration in a much more orderly manner, without the danger of phase segregation.

The above experimental mobility values are found to scale with the dendrimer hydrodynamic radius R estimated from gel permeation chromatography³⁵ according to $\mu \propto R^2 e^{-2R/R_0}$, where R_0 is a characteristic hopping distance and $2R$ corresponds to the minimum separation between two adjacent chromophores. This scaling is seen in Fig. 6. Such a dependence of mobility on intersite separation, which is a signature of polaronic hopping transport, has been observed by Gill³⁶ in molecularly doped polymers, where the distance R is defined by the dopant concentration in the blend. A value of 0.39 nm is found here for R_0 from the mobility measurements, which compares to 0.5 nm for trinitrofluorenone poly-vinylcarbazole blends.³⁶

The inverse of the external quantum efficiency is also plotted in the same scaling in Fig. 6, yielding an R_0 of 0.45 nm, which is very close to the scaling of the mobility. The remarkable similarity of scaling suggests that the increase in efficiency with increasing generation is due primarily to a reduction in hole mobility. However, the increase in efficiency suggests that there is no corresponding reduction in electron mobility. It appears that the effect of the increased separation between chromophores on the electron current is more complicated due to the possibility of electron trapping resulting from the differences in the core and dendron lowest unoccupied molecular orbital levels. One interpretation of the correlation between increased efficiency and reduced hole mobility is that electrons are more readily trapped on the chromophores than holes, as has previously been suggested for PPV-based devices.³⁷ The device operation may be understood in terms of mobile holes meeting up with trapped electrons. Although the device operation involves many factors, the scaling of mobility and efficiency with

TABLE I. Fitting parameters obtained by fitting to IV characteristics in Fig. 3 using the device model (Ref. 39).

	G0	G1	G2	G3
Barrier height (eV)	0.47	0.48	0.48	0.49
μ_0 (cm ² /Vs)	5.1×10^{-6}	3.4×10^{-6}	6.2×10^{-9}	5.5×10^{-9}
E_0 (V/cm)	7.3×10^4	9.6×10^4	2.1×10^4	3.3×10^4

dendrimer radius provides evidence that for the case of aluminum electrodes the efficiency is determined by the reciprocal of the hole mobility.

C. Device model

We move on now to discuss a numerical model of the observed device properties. Conjugated dendrimers provide ideal systems in which to study the microscopic nature of charge transport in organic semiconductors. The control of mobility can be used to test device models that describe the operation of polymer LEDs.^{21,29,38–41} A model that has been widely used was developed by Davids, Campbell, and Smith.³⁸ It uses a combination of thermionic emission and tunneling currents to describe the injection of charge carriers over a barrier that then give the charge-carrier density at the electrode. The coupled Poisson, drift and continuity equations are then solved across the device using a field dependent mobility of the form $\mu_{(E)} = \mu_0 e^{\sqrt{E}E_0}$, where μ_0 and E_0 relate to material parameters. Good quality fits have previously been achieved with this model and mobility parameters determined in MEH-PPV devices were found to agree well with those obtained from TOF measurements on the identical structure at room temperature.²⁹ We have previously described a modification of this model to calculate the temperature dependence of LEDs, as well as the effect of oxidation on the mobility.³⁹ In the following, we use the model to investigate the properties of the dendrimer LEDs. As seen in Fig. 3, current-electric field characteristics of devices of different generations with ITO/PEDOT and aluminum electrodes move to higher fields with increasing generation. The lines in Fig. 3 show model fits to the data using the barrier height and the parameters μ_0 and E_0 as fitting parameters. The fits qualitatively follow the shape of the current-voltage characteristics and quantitatively describe the measured current. At lower fields, there are some deviations due to the influence of space charge on carrier injection, which is not incorporated into the model. The feature at 0.4 MV/cm in G0 is associated with relatively poor stability and was observed for a number of G0 devices, but not for higher generation LEDs. The model fitting parameters are summarized in Table I.

Remarkably, the obtained mobility values of the form given by the above equation agree very well with the values determined through TOF, as is seen in Fig. 5. This is good evidence that the model gives a qualitatively useful and reasonable description of the physical processes involved in device operation for these molecules. The barrier height is determined as ~ 0.47 eV, which is a reasonable value for hole injection into a green-blue emitter on a PEDOT layer.^{42,43}

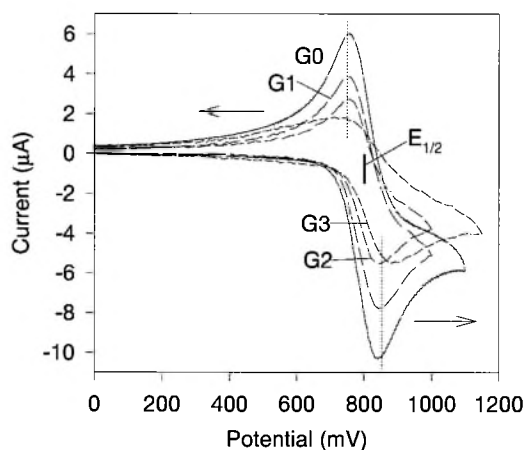


FIG. 7. Cyclic voltammety of dendrimer solutions of concentration 1.0 mmol/l in tetrabutylammonium hexafluorophosphate (0.1 mol/l) in dichloromethane versus Ag/AgCl/3M NaCl. The dashed lines mark the anodic and cathodic peaks, respectively. The $E_{1/2}$ values are marked by the bold line.

The value of the barrier height obtained in the fits is effectively independent of generation, which suggests that injection takes place into the core of the dendrimer. The electronic properties of the core, hence, remain unaffected by further branching of the dendrons. This was confirmed by electrochemistry, where the same oxidation potential was observed for all four dendrimers. Cyclic voltammety was performed on dendrimer solutions of concentration 1.0 mmol/l in tetrabutylammonium hexafluorophosphate (0.1 mol/l) in dichloromethane. Previous measurements on related compounds also showed that the dendrimer generation had little effect on the $E_{1/2}$ of the core.³⁵ As seen in Fig. 7, the oxidation traces show very little dependence on generation. The $E_{1/2}$ points, which are defined as the midpoints between the cathodic and anodic peaks, were found to be 800 mV [relative to Ag/AgCl/3M NaCl (Ref. 35)] for all four generations. This demonstrates clearly that the energy levels of the chromophore remain unaffected by further branching of the dendrons. The results obtained from cyclic voltammety are, hence, in excellent agreement with our model calculations on dendrimer LEDs, demonstrating that the barrier to injection is independent of dendrimer generation.

In summary, we have shown that by controlled variation of a device parameter, namely the mobility, the parameter space of physical models for LEDs may be explored in a further dimension, alongside the barrier height,⁴⁰ intense electrical operation,⁴¹ photo-oxidation,³⁹ and temperature.³⁹

D. Turn-on dynamics of LEDs

Our control of the mobility can also be used to understand the processes involved in pulsed operation of LEDs. The origin of the delay and rise time of EL in LEDs is currently a matter of debate: it has been proposed that it is due to the charge-carrier mobility,^{44–47} a signature of dispersive transport;⁴⁸ or merely the buildup of space charge in the device.⁴⁹ In contrast, optical measurements of the charge carrier density in LEDs were found not to correlate with results

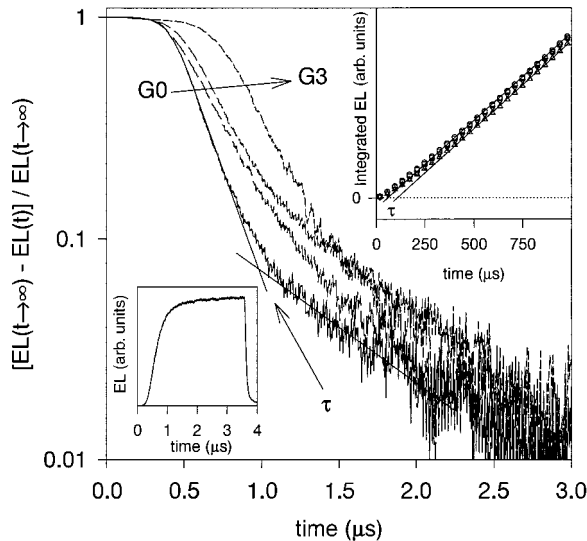


FIG. 8. Transient EL traces for a $3.5 \mu\text{s}$ pulse at an electric field of 2.5 MV/cm . As the generation is increased, there is a small change in the onset of EL. An analysis following Ref. 47 does not yield transit times vastly dependent on generation. The lower inset shows a typical trace for a G1 LED. The upper inset displays the integrated emission for a 1 ms pulse at a field of 1.8 MV/cm as a function of time—the intersection with the time axis determines the transit time (Ref. 48).

from transient EL.⁵⁰ The question of the origin of the delay and rise time in EL is of great interest, as the pulsed operation of LEDs is extremely important for both passively addressed matrix displays, as well as in the search for electrically driven polymer lasing. In addition, transient EL has frequently been used to infer mobility values,^{44–47} although few attempts have been made to find a correlation^{45,46,50} with values obtained from more direct measurements such as TOF. The mobility in our dendrimers changes by two orders of magnitude, so we can establish the effect of charge-carrier mobility on transient EL by investigating the generation dependence.

The analysis of a transient EL signal is shown in Fig. 8 on a logarithmic scale. A typical transient of a G1 LED driven for $3.5 \mu\text{s}$ at an electric field of 2.5 MV/cm is shown in the lower inset. (Note that this field is larger than the field in Fig. 3 due to the absence of the PEDOT layer.) There is a slight shift towards longer delay times with increasing generation. Following the analysis of Pinner, Friend, and Tessler,⁴⁷ it should be possible to determine a mobility from the intersection of the two straight lines describing the initial rise and the more gradual approach to the final value of luminescence, as shown in Fig. 8 and marked by τ . As the generation number is increased, this time τ increases by less than a factor of 2, in contrast to the two orders of magnitude observed in the transient photocurrent measurements. Also, a reduction in temperature (not shown) was found to have no systematic effect on the transient response, with the change in τ less than a factor of two over the temperature range from 300 to 80 K. As the mobility is strongly thermally activated, a delay time governed by the mobility would be expected to increase

by orders of magnitude with decreasing temperature, as has been shown (for example) in the polymer MEH-PPV,^{39,51} but is not observed here.

A further analysis of transient EL data is shown in the upper inset of Fig. 8 for a 1 ms pulse at a field of 1.8 MV/cm . Following Blom and Vissenberg,⁴⁸ the transit time can be interpolated from the integral of the light emission. Blom and Vissenberg have used this analysis to conclude that the transport is dispersive and mobility values cannot be deduced from the transient EL. However, comparisons with photocurrent transients are not given. We find, as above, that the increase with generation is only by roughly a factor of 2, which is incompatible with the 2 orders of magnitude change in transit time seen in the transient photocurrent. This result shows that there are great dangers involved in attempting to deduce transit times and mobility values from transient EL and that due to the presence of both charge carriers, as well as injecting contacts and possible trapping sites, transient EL is an inherently complicated process. A possible qualitative explanation of the present observations is that the response of LEDs to a voltage pulse is primarily due to space charge and trapping effects⁴⁹ that appear to give rise to a virtually mobility independent recombination time of the fastest charge carriers.

Dispersion⁴⁸ apparently plays an important role, but the absence of any strong variation of transit time with generation in Fig. 8 in comparison to the change of mobility with generation as seen in Fig. 5 suggests that transient EL should be seen as a macroscopic probe of the device properties rather than a microscopic probe of the mobility. To this end, it is important to note that despite the low mobilities observed in these materials, EL turn on is seen within $1 \mu\text{s}$ for all materials, which demonstrates that these materials are suited to passive matrix display applications.

E. Balancing mobilities in bilayer devices

Our dendrimer system provides an elegant way of tuning the mobility without changing the energy gap of the material. This is achieved in a single molecule without the need for dilution and associated problems of phase segregation. The dendrimer family, hence, lends itself ideally as an emissive or nonemissive transport layer to multilayer LEDs. We explored this by vacuum depositing an electron transporting layer (50 nm) of either Alq_3 or PBD on top of the dendrimer ($\sim 80 \text{ nm}$) and completing the device with an evaporated magnesium-aluminum cathode. For devices containing Alq_3 , emission was seen from this layer, whereas for the PBD device dendrimer luminescence was observed. As is seen in the device characteristics in Fig. 9, the choice of both hole transporter, as well as electron transporter, has substantial impact on the device operation. The maximal sustainable current was measured for the Alq_3 device with the G0 dendrimer, which also exhibited the lowest turn-on voltage. Using the G3 dendrimer resulted in a decrease in current and a slight increase in efficiency. In contrast, the PBD devices supported less current than the single-layer device, although light emission was observed above a bias of 6 V in all cases. Again, the G3 device current was reduced with respect to the

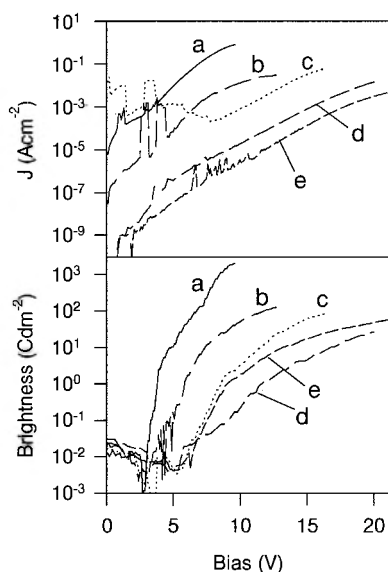


FIG. 9. Current voltage and brightness voltage for single layer and bilayer devices with MgAl electrodes. (a) G0/Alq₃, (b) G3/Alq₃, (c) G3, (d) G0/PBD, (e) G3/PBD.

G0 device, but the light output closely followed that of the single-layer device. The net result for bilayer devices containing the G3 dendrimer is a much improved device efficiency at very low brightnesses, which we estimate to be in the order of 10 Cd/A. Due to the low lying highest occupied molecular orbital level of PBD with respect to that of the dendrimer and the low charge-carrier mobility in the dendrimer, strong carrier confinement of charge carriers at the interface between the two materials is achieved. At higher brightnesses, the G3/PBD device was found to have an external quantum efficiency of approx. 0.4% (1 Cd/A). This application demonstrates that tuning of the mobility is an extremely useful property in order to construct well-balanced devices.

IV. CONCLUSIONS

We have demonstrated control of mobility over two orders of magnitude in a material for organic LEDs. The reduction in mobility with increasing generation can be related directly to a reduction in intermolecular interactions that also explains a decrease of the red emission tail of dendrimer films. The control of mobility allows a detailed study of the physical processes that govern the operation of LEDs. In particular, we find that the idea of describing LEDs by a superposition of injection and transport terms gives mobility values in agreement with those obtained from transient photocurrent measurements. The mobility is found to scale with dendrimer radius, signifying the hopping nature of transport in polymeric materials. We find that transient EL of these devices is not governed by the charge-carrier mobility.

The control of mobility is an extremely powerful tool when designing materials for specific applications. High mobilities in organic EL materials are not required for low brightness efficient backlights. Indeed, in a recent study Blom *et al.* demonstrated that, depending on the operating brightness required of the LED, the power efficiency may be optimized by changing the mobility.⁵² We have shown that the dendrimers can be used in a variety of LED configurations, where the device properties and efficiency can be tuned by the dendrimer generation.

ACKNOWLEDGMENTS

We thank D. G. Moon and O. Salata for assistance with measurements on bilayer LED's and K. Book and C. Im for helpful discussion. We acknowledge financial assistance from the Royal Society, Raychem Ltd., Opsy Ltd. (a CASE Award to MJF) and the German Academic Exchange Service (JML).

*Corresponding author: idws@st-andrews.ac.uk

¹C. W. Tang and S. A. Van Slyke, *Appl. Phys. Lett.* **51**, 913 (1987).

²J. H. Burroughes, D. D. C. Bradley, A. R. Brown, R. N. Marks, K. Mackay, R. H. Friend, P. L. Burn, and A. B. Holmes, *Nature (London)* **347**, 539 (1990).

³R. H. Friend, R. W. Gymer, A. B. Holmes, J. H. Burroughes, R. N. Marks, C. Taliani, D. D. C. Bradley, D. A. Dos Santos, J. L. Brédas, M. Lögdlund, and W. R. Salaneck, *Nature (London)* **397**, 121 (1999).

⁴H. Sirringhaus, P. J. Brown, R. H. Friend, M. M. Nielsen, K. Bechgaard, B. M. W. Langeveld-Voss, A. J. H. Spiering, R. A. J. Janssen, E. W. Meijer, P. Herwig, and D. M. deLeeuw, *Nature (London)* **401**, 685 (1999).

⁵R. Österbacka, C. P. An, X. M. Jiang, and Z. V. Vardeny, *Science* **287**, 839 (2000).

⁶J. H. Schön, C. Kloc, A. Dodabalapur, and B. Batlogg, *Science* **289**, 599 (2000).

⁷J. H. Schön, S. Berg, C. Kloc, and B. Batlogg, *Science* **287**, 1022 (2000).

⁸H. Bässler, *Phys. Status Solidi B* **175**, 15 (1993).

⁹Y. N. Gartstein and E. M. Conwell, *Chem. Phys. Lett.* **245**, 351 (1995).

¹⁰H. C. F. Martens, P. W. M. Blom, and H. F. M. Schoo, *Phys. Rev. B* **61**, 7489 (2000).

¹¹Z. G. Yu, D. L. Smith, A. Saxena, R. L. Martin, and A. R. Bishop, *Phys. Rev. Lett.* **84**, 721 (2000).

¹²L. L. Miller, R. G. Duan, D. C. Tully, and D. A. Tomalia, *J. Am. Chem. Soc.* **119**, 507 (1997).

¹³J. Bettenhausen and P. Strohmriegel, *Adv. Mater.* **8**, 507 (1996).

¹⁴P. J. Dandliker, F. Diederich, M. Gross, C. B. Knobler, A. Louati, and E. M. Sanford, *Angew. Chem. Int. Ed. Engl.* **33**, 1739 (1994).

¹⁵P. W. Wang, Y. J. Liu, C. Devadoss, P. Bharathi, and J. S. Moore, *Adv. Mater.* **8**, 237 (1996); A. Adronov and J. M. J. Frechet, *Chem. Commun. (Cambridge)* **18**, 1701 (2000).

¹⁶Y. Shirota, Y. Kuwabara, H. Inada, T. Wakimoto, H. Nakada, Y. Yonemoto, S. Kawami, and K. Imai, *Appl. Phys. Lett.* **65**, 807 (1993).

- ¹⁷M. Halim, J. N. G. Pillow, I. D. W. Samuel, and P. L. Burn, *Adv. Mater.* **11**, 371 (1999).
- ¹⁸J. N. G. Pillow, M. Halim, J. M. Lupton, P. L. Burn, and I. D. W. Samuel, *Macromolecules* **32**, 5985 (1999).
- ¹⁹J. M. Lupton, L. R. Hemingway, I. D. W. Samuel, and P. L. Burn, *J. Mater. Chem.* **10**, 867 (2000).
- ²⁰R. Kopelman, M. Shortreed, Z. Y. Shi, W. H. Tan, Z. F. Xu, J. S. Moore, A. BarHaim, and J. Klafter, *Phys. Rev. Lett.* **78**, 1239 (1997).
- ²¹B. K. Crone, I. H. Campbell, P. S. Davids, D. L. Smith, C. J. Neef, and J. P. Ferraris, *J. Appl. Phys.* **86**, 5767 (1999).
- ²²A. N. Sobolev, V. K. Belsky, I. P. Romm, N. Y. Chernikova, and E. N. Guryanova, *Acta Crystallogr., Sect. C: Cryst. Struct. Commun.* **41**, 967 (1985).
- ²³H. Scherand E. W. Montroll, *Phys. Rev. B* **12**, 2455 (1975).
- ²⁴M. Pope and C. E. Swenberg, *Electronic Processes in Organic Crystals* (Oxford University, New York, 1982).
- ²⁵E. Lebedev, Th. Dittrich, V. Petrova-Koch, S. Karg, and W. Brütting, *Appl. Phys. Lett.* **71**, 2686 (1997).
- ²⁶H. Meyer, D. Haarer, H. Naarmann, and H. H. Hörhold, *Phys. Rev. B* **52**, 2587 (1995).
- ²⁷M. Gailberger and H. Bässler, *Phys. Rev. B* **44**, 8643 (1991).
- ²⁸D. Hertel, H. Bässler, U. Scherf, and H. H. Hörhold, *J. Chem. Phys.* **110**, 9214 (1999).
- ²⁹I. H. Campbell, D. L. Smith, C. J. Neef, and J. P. Ferraris, *Appl. Phys. Lett.* **74**, 2809 (1999).
- ³⁰J. Bondkowski, I. Bleyl, D. Haarer, and D. Adam, *Chem. Phys. Lett.* **283**, 207 (1998).
- ³¹S. A. Carter, M. Angelopoulos, S. Karg, P. J. Brock, and J. C. Scott, *Appl. Phys. Lett.* **70**, 2067 (1997).
- ³²S. A. Jenekhe and J. A. Osaheni, *Science* **265**, 765 (1994).
- ³³M. Yan, L. J. Rothberg, E. W. Kwock, and T. M. Miller, *Phys. Rev. Lett.* **75**, 1992 (1995).
- ³⁴I. D. W. Samuel, G. Rumbles, and R. H. Friend, in *Primary Photoexcitations in Conjugated Polymers: Molecular Exciton versus Semiconductor Band Model*, edited by N. S. Sariciftci (World Scientific, Singapore, 1997).
- ³⁵P. L. Burn, R. Beavington, M. J. Frampton, J. N. G. Pillow, M. Halim, J. M. Lupton, and I. D. W. Samuel, *Mater. Sci. Eng. B* (to be published).
- ³⁶W. Gill, *J. Appl. Phys.* **43**, 5033 (1972).
- ³⁷P. W. M. Blom, M. J. M. Dejong, and J. J. M. Vleggaar, *Appl. Phys. Lett.* **68**, 3308 (1996).
- ³⁸P. S. Davids, I. H. Campbell, and D. L. Smith, *J. Appl. Phys.* **82**, 6319 (1997).
- ³⁹J. M. Lupton and I. D. W. Samuel, *J. Phys. D* **32**, 2973 (1999).
- ⁴⁰I. H. Campbell, P. S. Davids, D. L. Smith, N. N. Barashkov, and J. P. Ferraris, *Appl. Phys. Lett.* **72**, 1863 (1998).
- ⁴¹I. H. Campbell, D. L. Smith, C. J. Neef, and J. P. Ferraris, *Appl. Phys. Lett.* **75**, 841 (1999).
- ⁴²T. M. Brown, J. S. Kim, R. H. Friend, F. Cacialli, R. Daik, and W. J. Feast, *Appl. Phys. Lett.* **75**, 1679 (1999).
- ⁴³M. J. Frampton, R. Beavington, J. M. Lupton, I. D. W. Samuel, and P. L. Burn, *Synth. Met.* (to be published).
- ⁴⁴S. Karg, V. Dyakonov, M. Meier, W. Riess, and G. Paasch, *Synth. Met.* **67**, 165 (1994).
- ⁴⁵S. Forero, P. H. Nguyen, W. Brütting, and M. Schwoerer, *Phys. Chem. Chem. Phys.* **1**, 1769 (1999).
- ⁴⁶P. Ranke, I. Bleyl, J. Simmerer, D. Haarer, A. Bacher, and H. W. Schmidt, *Appl. Phys. Lett.* **71**, 1332 (1997).
- ⁴⁷D. J. Pinner, R. H. Friend, and N. Tessler, *J. Appl. Phys.* **86**, 5116 (1999).
- ⁴⁸P. W. M. Blom and M. Vissenberg, *Phys. Rev. Lett.* **80**, 3819 (1998).
- ⁴⁹J. Pommerehne, H. Vestweber, Y. H. Tak, and H. Bässler, *Synth. Met.* **76**, 67 (1996).
- ⁵⁰M. Redecker, H. Bassler, and H. H. Hörhold, *J. Phys. Chem. B* **101**, 7398 (1997).
- ⁵¹L. Bozano, S. A. Carter, J. C. Scott, G. G. Malliaras, and P. J. Brock, *Appl. Phys. Lett.* **74**, 1132 (1999).
- ⁵²P. W. M. Blom, M. C. J. M. Vissenberg, J. N. Huiberts, H. C. F. Martens, and H. F. M. Schoo, *Appl. Phys. Lett.* **77**, 2057 (2000).